Electrical Transport Characteristics and Deep Level Transient Spectroscopy of Ni/V/n-InP Schottky Barrier Diodes

S.Sankar Naik, V.Rajagopal Reddy*

Department of Physics, Sri Venkateswara University, Tirupati-517502, India

We report on the temperature-dependent electrical characteristics and deep level transient spectroscopy (DLTS) of the Ni/V/n-InP Schottky diodes in the temperature range of 180-420 K. Current density - voltage (J-V) characteristics of these diodes have been analyzed on the basis of thermionic emission theory with Gaussian distribution model of barrier height. The calculated Schottky barrier height (ϕ_{bo}) and ideality factor (n) of Ni/V Schottky contact is in the range of 0.39 eV and 2.36 at 180 K, and 0.69 eV and 1.27 at 420 K, respectively. It is observed that the zero-bias barrier height increases while ideality factor decreases with increasing temperature. A ϕ_{bo} versus $q/2kT$ plot is drawn to obtain evidence of a Gaussian distribution of the barrier heights, and values of $\bar{\phi}_{bo} = 0.95$ eV and $\sigma_{c0} = 128$ eV for the mean barrier height and standard deviation. A modified Richardson plot gives $\bar{\phi}_{bo\ (T=0)} = 0.98$ eV and Richardson constant (A^*) = 7.068 A K^{-2}cm^{-2}. The discrepancy between Schottky barrier height (SBHs) estimated from J-V and C-V measurements is also discussed. Thus, it is concluded that the temperature dependence of J-V characteristics of the SBHs on n-InP can be explained on the basis of themionic emission mechanism with Gaussian distribution of the barrier heights. DLTS results showed that two deep levels are identified (E1 and E2) in as-grown sample having activation energies of 0.29 ± 0.01 and 0.69 ± 0.02 with capture cross-section 3.29×10^{-15} cm^2 and 5.85×10^{-17} cm^2 respectively.

Keywords: Ni/V/n-InP Schottky diode, Temperature-dependent electrical properties, Deep level defects, DLTS measurements.

PACS numbers: 73.30.+Y, 73.40.Ei, 73.61.Ey

1. INTRODUCTION

Due to direct transition band gap and high electron mobility of indium phosphide (InP), it is an attractive semiconductor material for the fabrication of high-speed semiconductor devices such as metal-semiconductor field effect transistors (MESFETs), opto-electronic and high-speed electronic device applications [1-2]. Determination of Schottky barrier height and other characteristic parameters of Schottky diode, the interface states can play an important role. These parameters can affect device performance, stability and reliability [3-4]. Due to technological importance of Schottky barrier diodes, a full understanding of the nature of conduction mechanism is of great interest [5]. Metal-semiconductor (MS) contact is one of the most widely used rectifying contacts in the electronics industry [1, 6-8]. The current density-voltage (J-V) characteristics of the MS contacts usually deviate from the ideal thermionic emission (TE) current model [8, 9-10]. Particularly, Schottky diodes (SDs) with low BHs have found applications in devices operating at cryogenic temperature as infrared detectors and sensors in thermal imaging [11-12]. Therefore, analysis of the J-V characteristics of the Schottky barrier diodes (SBDs) at room temperature only does not give detailed information about their conduction process or the nature of barrier formation at the M-S interface [13-14]. The temperature dependence of the J-V characteristics allows us to understand different aspects of conduction mechanisms across the metal/InP interface and the study of different effects, such as barrier inhomogeneities and surface state density on carrier transport at metal/InP Schottky barrier diode [15].

Most of the experimental and theoretical studies of the current flow mechanism in Schottky barriers have been reported in the literature [16-21]. For examples, Cetin et al. [16] fabricated Au/n-InP SBDs and studied the temperature dependent electrical characteristics in the temperature of 80-320 K. They reported that the barrier height (BH) and ideality factor (n) varied in the range of 0.274-0.516 eV and 2.32-1.05, respectively. Janardhanam et al. [17] studied the electrical transport characteristics of ruthenium/n-InP Schottky diode by I-V-T measurements, reported that the BH varied from 0.39 eV (at 200 K) to 0.60 eV (at 400 K). Soylu et al. [18] investigated the electrical characteristics of the Au Schottky contact on moderately doped n-type InP (Au/MD/n-InP) in the temperature range of 60-300 K. They found that the ideality factor n of the diode decreases while the zero-bias BHs increasing with increase in temperature. Nanda Kumar Reddy et al. [19] fabricated the Pt/Au/n-InP Schottky barrier diode and investigated I-V and C-V characteristics in the temperature range of 210-420 K. They showed that the barrier parameters vary significantly with temperature. Naik et al. [20] carried out the temperature dependent current-voltage and capacitance-voltage characteristics of the Au/Ni/n-InP SBDs in the temperature range of 210-420 K. They found that the decrease in ideality factor and increase in BH with increasing temperature such behavior had explained on the basis of thermionic emission (TE) with a Gaussian distribution of the BHs at the interface. Recently Subba Reddy et al. [21] studied the Schottky barrier parameters of Pd/Ti contacts on n-type InP by I-V-T and C-V-T measurements, reported that the barrier height (ϕ_{bo}), ideality factor (n) and series resistance (Rs) were strongly temperature dependent.

_____

* reddy_vrg@rediffmail.com

The deep level defects play a key role in controlling electrical properties of semiconductor material. The quality of the material in terms of device performance can be beneficial (or) detrimental strongly affected by deep levels due to impurities and native defects [22]. The nature of deep levels in InP is expected to be an important research area, especially if their role in the operation and characterization of semiconductor devices is to be understood. The presence of such deep levels, depending on the capture cross sections and density, may cause limitations in the performance and reliability of the InP devices. Deep level transient spectroscopy (DLTS) is an experimental tool for studying electrically active defects (known as charge carrier traps) in semiconductors [23]. DLTS investigates defects present in a space charge (depletion) region of a simple electronic device. The most commonly used are Schottky diodes or p-n junctions [24]. While several deep levels in InP have reported [25-29], the nature of these defects has received little attention. Zhao et al [30] studied the annihilation of deep level defects in InP through high temperature annealing by deep level transient spectroscopy (DLTS) and Thermally stimulated current spectroscopy (TSC) measurements. Recently Janardhanam et al. [31] investigated the deep level defect behavior in undoped n-InP after rapid thermal annealing using DLTS technique. In the present work, we report on the temperature-dependent electrical characteristics of Ni/V Schottky contacts and deep level defects in InP by DLTS technique. Also, the current transport mechanism and the nature of the defects are discussed based on the results.

2. EXPERIMENTAL DETAILS

Liquid Encapsulated Czoralski (LEC) grown undoped n-InP having a carrier concentration of 4.9 to 5.0×10^{15} cm^{-3} is used in the present work. The InP samples are first ultrasonically degreased with warm trichloroethylene followed by acetone and methanol for 5 minutes each to remove the contaminants. The samples are then etched with HF (49 %) and H_2O (1:10) to remove the native oxides from the surface of the substrate. Ohmic contact of thickness 700 Å is formed by thermal evaporation of indium (In) on the rough side of the InP wafer under a pressure of 6×10^{-6} mbar during the deposition. Then the samples are annealed at 350 °C for 1 min in N_2 atmosphere. Circular metal contacts of 0.7 mm diameter and 500 Å/500 Å thickness of Ni/V are deposited as a Schottky contact by means of electron beam evaporation on the polished side of the InP wafer through a stainless steal mask. The current density-voltage (J-V) and capacitance voltage (C-V) characteristics are measured in the temperature range of 180-420 K in steps of 40 K by using Keithly source measuring unit (2400) and automated deep level spectrometer (Semilab, DLS-83D). Also, DLTS measurements are performed in the temperature range 100-400 K by automated DLTS system (SEMI LAB, DLS-83D) by placing the sample inside the liquid-nitrogen cryostat to evaluate trap parameters. The DLS-83D uses lock-in amplifier and DLTS measurements are made with different lock-in frequencies of 40, 80 and 120 Hz. DLTS measurements are made with pulse du-

ration of 100 μs which is long enough to fill traps with a filling pulse voltage is + 0.5 V and reverse bias is – 4 V.

3. RESULTS AND DISCUSSION

3.1 Temperature-Dependent Characteristics of Ni/V Schottky Contacts

For a Schottky barrier diode, current transport is due to majority carriers and it may be described by thermionic emission (TE) over the interface barrier. TE current at the forward bias can be written as [5]

$$J = J_0 \exp\left(\frac{qV}{nkT}\right)\left[1 - \exp\left(-\frac{qV}{kT}\right)\right] \qquad (1)$$

where J_0 is the saturation current derived from the straight line intercept of ln$J$ at $V = 0$ and is given by

$$J_o = A^* T^2 \exp\left(-\frac{q\phi_{b0}}{kT}\right) \qquad (2)$$

where q is the electronic charge, V is the definite forward-bias voltage, A is the effective diode area, k is the Boltzmann's constant, T is the absolute temperature, A^* is the effective Richardson's constant of 9.4 Acm^{-2}K^{-2} for n-type InP [32], ϕ_{bo} is the zero bias effective barrier height and n is the ideality factor which is a measure of conformity of the diode to pure thermionic emission. The ideality factor n obtained from the slope of the forward bias ln$J$-V characteristics from Eq.(1) and it can be written as

$$n = \frac{q}{kT}\left(\frac{dV}{d(\ln J)}\right) \qquad (3)$$

The zero-bias barrier height (BH) and the ideality factor n of the Ni/V/n-InP SBD are calculated using Eq.(3) and (4) at each temperature respectively. Fig.1 shows the semilog J–V characteristics of the Ni/V/n-InP Schottky diodes at different temperatures

$$\phi_{bo} = \frac{kT}{q}\ln\left(\frac{A^* T^2}{J_0}\right) \qquad (4)$$

The zero-bias barrier height (BH) ϕ_{bo} and the ideality Eq.(3) and (4) at each temperature respectively. Fig.1 factor n of the Ni/V/n-InP SBD are calculated using shows the semilog J-V characteristics of the Ni/V/n-InP Schottky diodes at different temperatures.

The experimental values of n and ϕ_{bo} are determined from intercepts and slopes of the forward bias ln$J$ versus V plot at each temperature, respectively. Once J_0 is known, the zero bias barrier height can be computed with the help of Eq. (2). The calculated values of n and ϕ_{bo} for the Ni/V Schottky contact range from $n = 2.36$ and $\phi_{bo} = 0.39$ eV at 180 K, and $n = 1.27$ and $\phi_{bo} = 0.69$ eV at 420 K respectively. The ϕ_{bo} and n determined from semilog-forward J-V plots are found to be a strong function of temperature. It is observed that the ideality factor n decreases while the ϕ_{bo} increases with increase in temperature. Fig.2 shows the temperature dependence of the ideality factor n and the zero bias barrier height ϕ_{bo} of Ni/V Schottky contact.
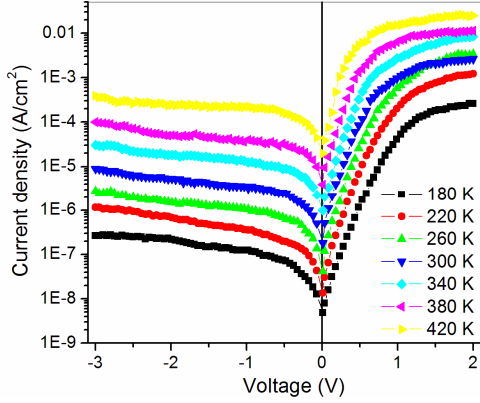
Fig. 1 – Experimental current density-voltage (J-V) characteristics of a Ni/V/n-InP Schottky contact at various temperatures

Such behavior for the ideality factor and the barrier height are attributed to the particular distribution of the interface states or an alternative approach to the lateral inhomogeneities that are found in the Schottky barrier interfaces. That is, the Schottky barrier consisted of laterally inhomogeneous patches of different barrier heights. The patch with lower barrier height yields a larger ideality factor and vice versa. Spatially inhomogeneous barrier height and the potential fluctuations at the interface that consist of the low and high barrier heights may cause the deviations in the ideality factor and barrier heights [18, 33-34]. So, the current through the diode will flow preferentially through the lower barriers in the potential distribution. At low temperatures the current transport across the metal/semiconductor interface is a temperature activated process, the current transport will be dominated by the current flowing through the patches of lower SBH and a larger ideality factor [33-34].
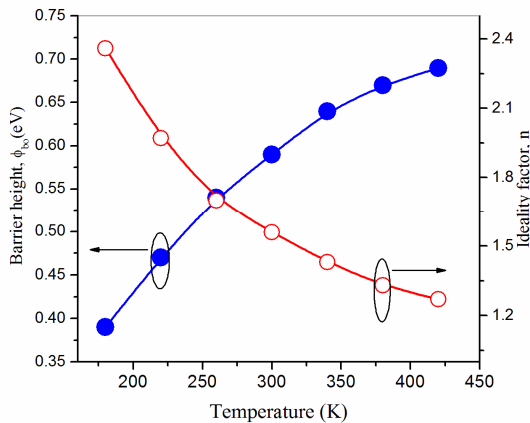

Fig. 2 – Temperature dependence of the ideality factor (the open circle) and barrier height (the filled circle) for the Ni/V Schottky contact

According to Eq. (2) (indicated by closed circle), a plot of conventional activation energies $\ln(J_0/T^2)$ versus $1/T$ plot is shown in Fig. 3. At low temperatures, an experimental $\ln(J_0/T^2)$ versus $1/T$ plot shows significant deviation from linearity. Bowing of the experimental $\ln(J_0/T^2)$ versus $1/T$ curve may be caused by the temperature dependence of the BH and ideality factor. This may be due to the existence of the surface inho-

mogeneities of the n-type InP substrate [35-36]. The commonly observed deviation in the Richardson plots, as will be discussed below, by assuming the effects of
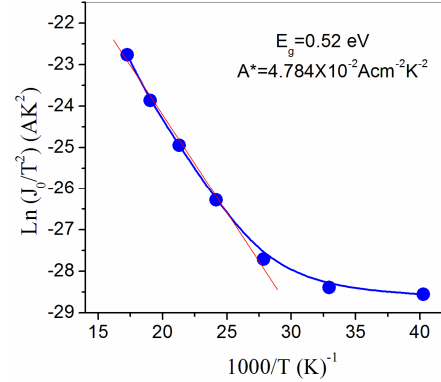

Fig. 3 – Richardson plots of the $\ln(J_0/T^2)$ versus $1/T$ plot (the closed circles) for Ni/V/n-InP Schottky diode

the image-force, the effect of tunnelling current through the potential barrier, the effect of recombination in the space charge region appearing at low voltage and the variation of the charge distribution near the interface [37]. From the linear portion of the experimental $\ln(J_0/T^2)$ versus $1/T$ plot, the activation energy is determined and the value is 0.52 eV. The value of A^* is obtained from the intercept of the straight line portion of the ordinate is equal to 4.784×10^{-2} $Acm^{-2}K^{-2}$ for InP.

The decrease in the BH and the increase in the ideality factor with a decrease in the measurements temperature are indicatives of a deviation from the pure TE theory and possibly the TFE mechanism may be considered. If current transport is controlled by TFE theory, the connection between the current density and voltage can be expressed by [5, 38]

$$I = I_s \exp\left[\frac{qV}{E_0}\right] \tag{5}$$

with

$$E_0 = E_{00} \coth\left[\frac{qE_{00}}{kT}\right] = \frac{nkT}{q} \tag{6}$$

where E_{00} is the characteristic energy that is related to the tunnel effect transmission probability

$$E_{00} = \frac{h}{4\pi}\left(\frac{N_d}{m_e^* \varepsilon_s}\right)^{\frac{1}{2}} \tag{7}$$

where $h = 6.626 \times 10^{-34}$ $J.sec$, N_d is the donor concentration, ε_s is the semiconductor dielectric constant and m_e^* is the electron effective mass. In the case of our Ni/V/n-InP Schottky barrier diode with $N_d = 4.9 - 5.0 \times 10^{15}$ cm^{-3}, $m_e^* = 0.077$ m_0 and $\varepsilon_s = 12.4$ ε_0 [39], the value of E_{00} is found to be about 1.365 mV. When considering the bias coefficient of the barrier height, $\beta = \partial \varphi_b / \partial V$ Eq. (6) can be written as [40]

$$n_{tun} = \frac{E_0}{kT(1-\beta)}. \tag{8}$$

When the current through Schottky junction is dominated by TFE, the variation of the ideality factor with temperature presented for different characteristic energy values of E_{00} are shown in Fig. 4. The solid lines (Fig. 4) are obtained by fitting Eq. (6) without considering the bias coefficient of the barrier height, $\beta = 0$, for the Ni/V/n-InP SBD. The filled circles in the Fig. 4 shows the temperature dependence values of ideality factor obtained from the experimental current density-voltage (J-V) characteristics.
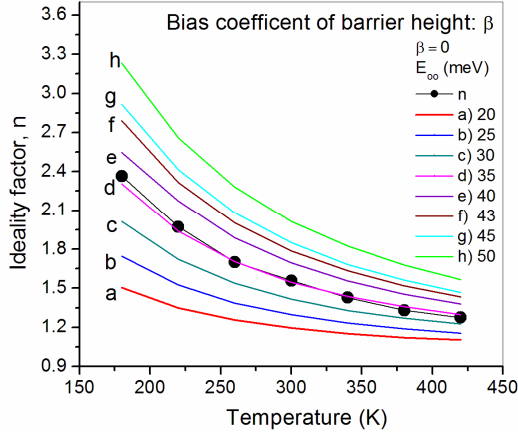

Fig. 4 – Theoretical temperature dependence of ideality factor according to Eq. (8), the bias coefficient of barrier height, $\beta = 0$, the closed circles show the experimental temperature dependence values of ideality factor obtained from the current density-voltage (J-V) characteristics

From the Fig. 4, it is observed that the experimental temperature dependence of ideality factor is in agreement with the curve (d) obtained with $E_{00} = 49$ mV for the Ni/V/n-InP diode. According to Tung [38], the behavior usually attributed to the TFE is not necessarily the conduction mechanism even though tunneling should dominate the electron conduction at heavily doped metal-semiconductor contacts, whenever an ideality factor dependence like that in Fig. 4 is observed. Generally varying dependencies of the ideality factor can originate from the same transport mechanism, e.g., thermionic emission when the SBH is inhomogeneous. These facts do not imply that the conduction mechanism at the Schottky barrier diodes is exclusively thermionic emission, but rather than the ideality factor dependency. This cannot be used as the only criterion for the determination of conduction mechanism.

The theoretically calculated value of 1.365 mV for n-InP is less than the characteristic energy value E_{00} value. The possible origin of the high characteristic energy values E_{00}, it should be underlined that E_{00} is connected with the transmission probability [41-42]. The characteristic energy has been related to several effects such as the electric field present on the surface of the semiconductor [43], the existence of relatively a thick interfacial insulating layer between the deposited metal and semiconductor and the density of states. Therefore, any mechanism which enhances the electric field or the density of states at the semiconductor surface will increase the TFE and so the apparent E_{00}.

According to Song et al [18] and Werner and Guttler [44], the increase in the barrier height with a increase in temperature can also be explained by the lateral

distribution of BH if the barrier height has a Gaussian distribution of the barrier height values over the Schottky contact area with the mean barrier height ($\bar{\phi}_{b0}$) and standard deviation σ_{s0}. The Gaussian distribution of the BHs yields the following expression for the BH [45-46]

$$\phi_{bo} = \bar{\phi}_{b0}(T = 0) - \frac{q\sigma_{s0}^2}{2kT} \qquad (9)$$

where $\bar{\phi}_{b0}$ and σ_{s0} are the mean barrier height and its standard deviation at the zero bias, respectively. The temperature dependence of σ_{s0} is usually small and can be neglected. The observed variation of ideality factor with temperature in the model is given by [44]

$$\left(\frac{1}{n_{ap}} - 1\right) = \rho_2 - \frac{q\rho_3}{2kT} \qquad (10)$$

where n_{ap} is apparent ideality factor (experimental data) and the coefficients ρ_2 and ρ_3 quantify the voltage deformation of the BH distribution, namely, the voltage dependencies of the mean BH and the barrier distribution widths are given by coefficients ρ_2 and ρ_3, respectively. The Fig. 5 shows the plot of $\bar{\phi}_{b0}$ versus $1/2kT$ which is a straight line with the intercept on the ordinate determining the mean barrier height $\bar{\phi}_{b0}$ and the slope gives the standard deviation σ_{s0}. The obtained values are 0.95 eV and 128 mV for $\bar{\phi}_{b0}$ and σ_{s0} respectively. The experimental results of $\bar{\phi}_{b0}$ fit very well with the theoretical. When comparing the $\bar{\phi}_{b0}$ and σ_{s0} parameters, it is seen that the standard deviation is $\approx 14.1\%$ of the mean barrier height. The standard deviation is a measure of the barrier homogeneity. The lower value of σ_{s0} indicates to more homogenous barrier height. The obtained value of $\sigma_{s0} = 128$ mV is not small compared to the mean value of $\bar{\phi}_{b0} = 0.95$ eV and it indicates the presence of larger inhomogeneities at the interface of Ni/V Schottky contact.
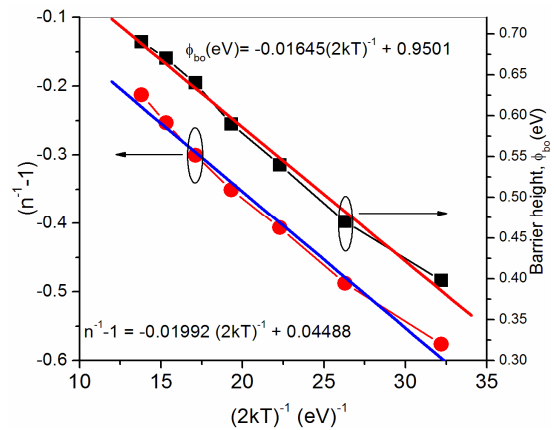

Fig. 5 – Zero-bias barrier height and ideality factor versus $1/(2kT)$ curves of the Ni/V/n-InP Schottky diode according to Gaussian distributions of the barrier height

As stated earlier, the conventional activation energy $\ln(J_0/T^2)$ versus $1/T$ plot has showed nonlinearity at

low temperatures (Fig. 3). To explain these discrepancies, according to the Gaussian distribution of the BH, we get

$$\ln\left(\frac{J_0}{T^2}\right) - \left(\frac{q^2\sigma_{so}^2}{2k^2T^2}\right) = \ln(A^*) - \frac{q\bar{\phi}_{b0}}{kT}. \quad (11)$$

According to Eq. (11), a modified $\ln(J_0/T^2)$-$(q^2\sigma_{s0}^2/2k^2T^2)$ versus $10^3/T$ plot can be obtained. The plot should give a straight line with the slope directly yielding the mean barrier height $\bar{\phi}_{b0}$ $(T = 0)$ and the intercept $(\ln A^*)$ at the ordinate, determining A^* for a given diode area A. As can be seen from Fig. 6, the modified Richardson plot has a quite good linearity over the whole temperature range corresponding to single activation energy around mean BH. The intercept at the ordinate of the modified $\ln(J_0/T^2)$-$\left(q^2\sigma_{so}^2/2k^2T^2\right)$ versus $1000/T$ plot gives the Richardson constant (A^*) as $7.068\,\text{AK}^{-2}\text{cm}^{-2}$, respectively, without using the temperature coefficient of the barrier height. The obtained Richardson constant value is in close agreement with the known value of $9.4\,\text{AK}^{-2}\text{cm}^{-2}$ for n-type InP. The mean BH value of 0.98 eV determined from the slope of the Richardson plot is regard as the effective barrier height. This value of $\bar{\phi}_{b0}$ $(T = 0) = 0.98$ eV is approximately the same as the value of $\bar{\phi}_{b0}$ $(T = 0) = 0.95$ eV from the plot of ϕ_{ap} versus $(1/2kT)$ given in Fig. 5.
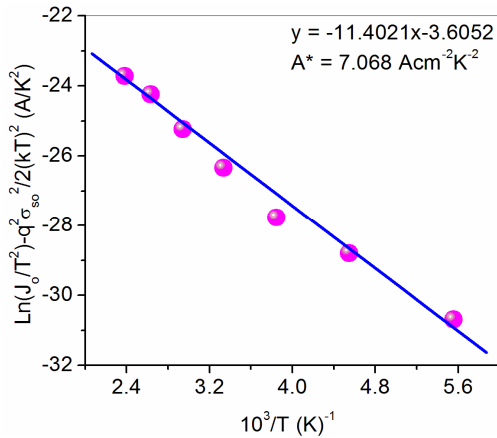

Fig. 6 − Modified Richardson plot $\ln(J_0/T^2)$ - $\left(q^2\sigma_{so}^2/2k^2T^2\right)$ versus $1/T$ plot for the Ni/V Schottky contact according to Gaussian distribution of the barrier heights

The experimental reverse bias C^{-2}-V characteristics of the Ni/V Schottky contacts over the temperature range $180 - 420$ K in steps of 40 K are shown in Fig. 7. The junction capacitance has been measured at a frequency of 1 MHz. In Schottky diodes, the depletion layer capacitance is given as [3]

$$\frac{1}{C^2} = \left(\frac{2}{\varepsilon_s q N_d A^2}\right)\left(V_{bi} - \frac{kT}{q} - V\right) \quad (12)$$

where ε_s is the permittivity of the semiconductor $(\varepsilon_s = 12.4\ \varepsilon_0)$, V is the applied voltage. The x-intercept of the plot of $(1/C^2)$ versus V gives V_0 and it is related to the

built in potential V_{bi} by the equation $V_{bi} = V_0 + kT/q$, where T is the absolute temperature. The barrier height is given by the equation $\phi_{(C-V)} = V_0 + V_n + kT/q$, here $V_n = (kT/q)\ln(N_c/N_d)$. The density of states in the conduction band edge is given by $N_c = 2(2\pi m^*kT/h^2)^{3/2}$, where $m^* = 0.078\ m_0$ and its value is $5.7 \times 10^{17}\text{cm}^{-3}$ for InP at room temperature [38]. The temperature dependence of the experimental donor concentration (N_d) is calculated from the slope of reverse bias C^{-2}-V characteristics (Fig. 8). The calculated values of N_d are in the range 4.129×10^{15} to 4.999×10^{15} cm^{-3} in the temperature range of $180 - 420$ K. It is noted that the donor concentration of the Ni/V Schottky contact decreases with decrease in temperature. The estimated Schottky barrier height of Ni/V Schottky contact is in the range of 0.96 eV at 180 K to 0.71 eV at 420 K respectively (The calculated BHs and ideality factor shown in Table 1).

As pointed out by Zhu et al [47], due to the square dependence of $\phi_{(C-V)}$ on $1/C$ compared to the logarithmic dependence of ϕ_{bo} on the current, $\phi_{(C-V)}$ is more sensitive to the experimental errors of the measured data than ϕ_{bo}. It is seen from Fig.7 that the barrier height $\phi_{(C-V)}$ increases with decrease in temperature.

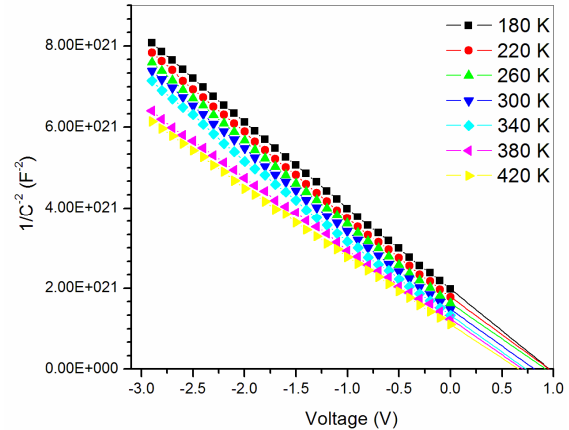**Fig. 7** − The reverse bias C^{-2}-V characteristics of the Ni/V Schottky contact at different temperatures in the range 180-420 K

Table 1 − The experimentally obtained electrical parameters of Ni/V Schottky contacts on n-type InP in the temperature range $180 - 420$ K

Temperature (K)	SBHs (eV)		Ideality Factor (n)
	J-V	C-V	
180 K	0.39	0.96	2.36
220 K	0.47	0.93	1.97
260 K	0.54	0.89	1.70
300 K	0.59	0.83	1.56
340 K	0.64	0.78	1.43
380 K	0.67	0.73	1.33
420 K	0.69	0.71	1.27

The temperature dependence of $\phi_{(C-V)}$ is expressed as

$$\phi_{(C-V)} = \phi_{(C-V)}(T = 0) + \alpha T \quad (13)$$

where $\phi_{(C-V)}$ $(T = 0$ K) is the barrier height extrapolated to zero temperature and α is the temperature coefficient

of the barrier height. Fitting of the experimental data from in Fig. 9 into Eq. (13) gives $\alpha = 1.15 \times 10^{-3}$ eV/K which is temperature coefficient of the InP band gap [48] and $\phi_{(C-V)}$ ($T = 0$ K) = 1.107 eV. As can be seen in Fig. 9, it is noted that the $\phi_{(C-V)}$ values are seen to be higher than the ϕ_{bo} values in investigated temperature range.
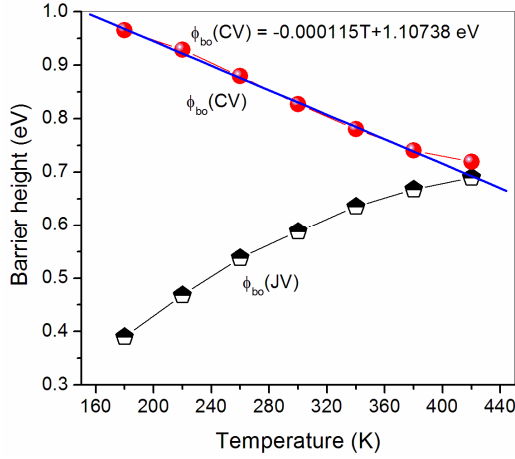

Fig. 8 − Variation of the zero-bias barrier height and C-V barrier height of Ni/V/n-InP Schottky diode

For the differences in BH values, some authors have been mentioned general reasons in the literature such as surface contamination at the interface, deep impurity levels, an intervening insulating layer, image force lowering and edge leakage currents [38, 49]. By assuming a Gaussian distribution of BHs with mean value $\bar{\phi}_{b0}$ and standard deviation σ_{s0} can also be used to explain the difference between $\phi_{(J-V)}$ and $\phi_{(C-V)}$ as well as the strong temperature dependence of $\phi_{(J-V)}$ and n at low temperature.
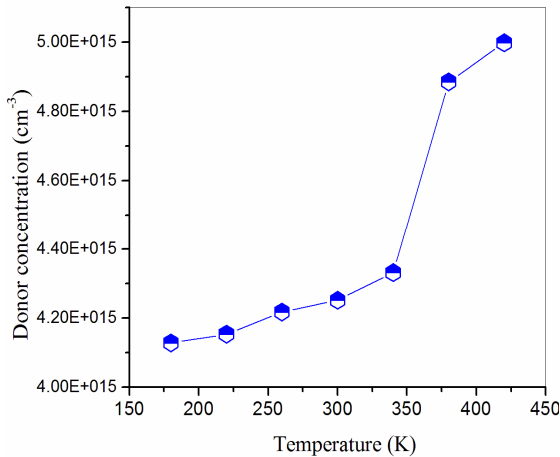

Fig. 9 − Temperature dependence of the donor concentration from reverse-bias C^{-2}-V characteristics for Ni/V Schottky contacts on n-InP

The capacitance depends only on the mean band bending and is insensitive to the standard deviation σ_{s0} of the barrier distribution [44]. The relation between $\phi_{(C-V)}$ and $\phi_{(J-V)}$ is given by

$$\phi_{(C-V)} - \phi_{(J-V)} = \frac{q\sigma_0^2}{2kT} + \frac{q\alpha_\sigma}{2k} \quad (14)$$

where α_σ is attributed to the temperature dependence of σ_0.

According to Eq. (14), the experimental ($\phi_{(C-V)} - \phi_{(J-V)}$) versus $1/2kT$ plot is shown in Fig. 10. The plot must give a straight line of slope $\sigma_0^2/2k$ and y-axis intercept $\alpha_\sigma/2k$ from which the parameters σ_0 and α_σ can be determined. The slope and y-axis intercept of the plot gives the values of $\sigma_0 = 157$ mV and $\alpha_\sigma = -5.3904 \times 10^{-5}$ V²K⁻¹,
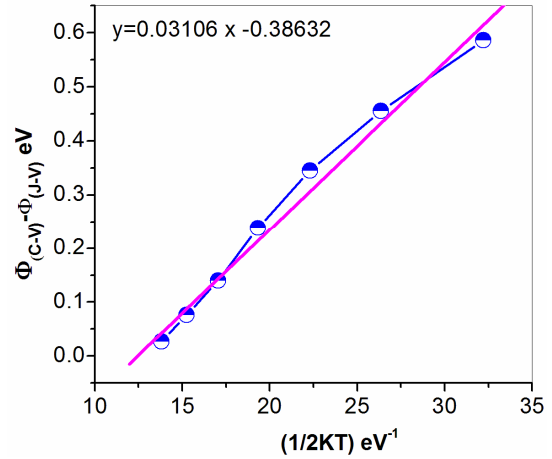

Fig. 10 − Barrier height difference between values as derived from the conventional evaluation of J-V and C-V data as a function of inverse temperature

respectively. This value of σ_0 is in close agreement with the value of $\sigma_{s0} = 128$ mV from the plot of $\bar{\phi}_{bo}$ versus $1/2kT$ drawn according to Eq. (9). Therefore, the spatial inhomogeneity of the Schottky barrier heights is not neglected in the analysis of electrical measurements.

3.2 Deep Level Transient Spectroscopy of Ni/V/n-InP Schottky Diode

In order to characterize the deep level defects, DLTS measurements are performed over the temperature range 100-400 K using automated DLTS system. Typically, a quiescent reverse bias of $V_r = -4$ V was employed with filling − pulse voltage $V_p = +0.5$ V and filling pulse width $t_p = 100$ μs. Any deep level can be experienced as either capture or emission of carrier, with transition probabilities per unit time depending on the free carrier concentrations, capture cross section of the trap, ionization energy and temperature. According to the value of applied voltage for the electron trap studied here in the space charge zone of Schottky diode on n-type InP, either emission or capture of electrons toward or from the bottom E_c of the conduction band is relevant. When the Fermi level just coincides with the trap level E_T, the capture coefficient equals the emission rate e_n resulting at equilibrium which is given by [50]

$$e_n = \sigma_n V_{th} N_c \exp\left(\frac{E_T - E_C}{kT}\right) = \frac{1}{\tau_e} \quad (15)$$

here σ_n is the capture cross-section, v_{th} is the thermal velocity of an electron defined as $V_{th} = (3kT/m_{eff})^{1/2}$, N_C is

the effective density of states at the bottom of the conduction band, k is the Boltzmann's constant and T is the absolute temperature and τ_e is the emission time constant which is the reciprocal of the emission time e_n.

Fig. 11 shows DLTS spectrum measured with lock-in frequency of 120 Hz. Two prominent deep levels are
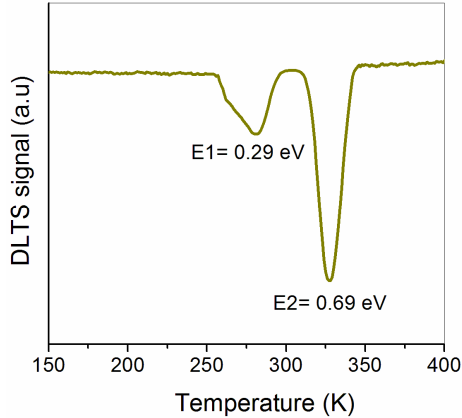

Fig. 11 – DLTS spectrum for Ni/V/n-InP Schottky diode. The rate window is 8.3 ms^{-1} and the filling pulse duration was 100 μs

observed in the as-grown InP that peaked at 281 K and 327 K and labeled as E1 and E2. The thermal activation energy for electron emission from each deep level is determined from an Arrhenius analysis of the emission time constant. From several such spectra, the product $e^{-1}{}_n v_{th} N_C$ can be calculated and plotted as function of 1000/T, leading usually to the straight line in an Arrhenius plot. An Arrhenious plot for two deep levels (281 K and 327 K) is shown in Fig. 12. The activation energies are determined from Fig. 12 for E1 and E2 are 0.29 ± 0.01 eV and 0.69 ± 0.02. We interpreted the E1 as corresponding to defect level with activation energy of 0.29 eV which is fairly similar to that reported by Lim et al [51], showing a defect level at 0.33 eV in undoped vapor phase epitaxy grown InP, McAfee et al. [52] shown a defect level at 0.35 eV in LEC grown InP under different diffusion conditions. The trap observed at E1 (0.29 eV) may be identified with trap RT2 (0.31 eV) reported by Kadoun et al. [53] using photo induced current spectroscopy. They suggest that this trap is attributed to V_P related intrinsic donor level.
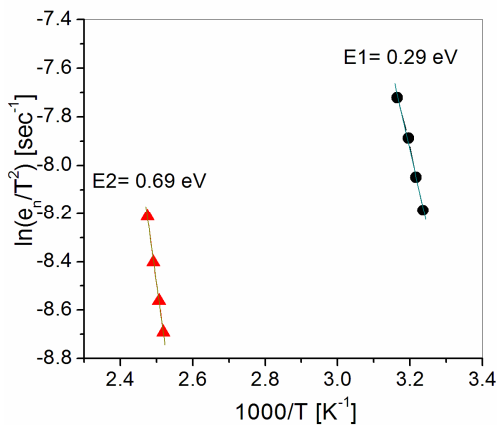

Fig. 12 – Arrhenius plots of the emission rate and temperature for Ni/V/n-InP Schottky diode

Similarly is our deep level E2 (0.69 eV) as corresponding to the 0.65 eV level reported by Zhao et al [54] by photocurrent spectroscopy in undoped LEC grown InP and attributed it to phosphorus antisite P_{In} defect. Shi et al [55] observed a deep level C (0.675 eV) in the room temperature metal/n-InP Schottky interfaces, which could be due to interface state trap. From these reports, the trap E2 (0.69 eV) observed in as-deposited Ni/V/n-InP Schottky contact, may be attributed to the phosphorus antisite defect P_{In}.

The carrier capture cross-section of semiconductor deep level defect contains useful information on the nature of the defect.
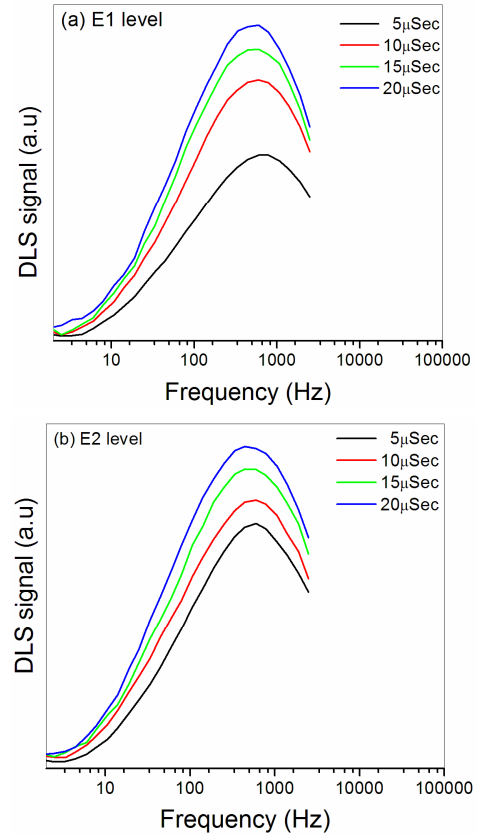

Fig. 13 – Capture cross-section measurement of DLTS spectra for Ni/V/n-InP Schottky diode

This parameter directly determined by measuring the capture time constant τ_c of the deep level [56]

$$\tau_c = \frac{1}{\sigma_n v_{th} n}, \qquad (16)$$

where σ_n is the cross-section, v_{th} is the thermal velocity of electron and n is the free carrier concentration at the measurement temperature. τ_c is often measured by monitoring the deep level transient spectroscopy (DLTS) peak height as a function of filling pulse width t_p [57] as shown in Fig. 13(a)-(b), respectively.

The slope of the plot $\ln(1 - N(t_p) / N_T)$ versus t_p giving τ_c^{-1}, where $N(t_p)/N_T$ is the peak amplitude. Fig. 14 (a)-(b) show the plot $\ln(1 - N(t_p)/N_T)$ versus t_p corresponding to E1 and E2 levels. Usually these plots
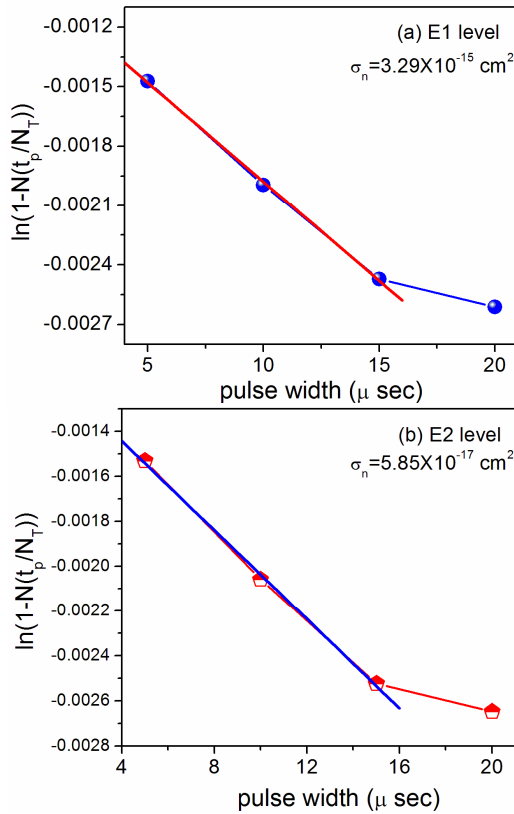
Fig. 14 – The capture cross-section plot of $\ln(1 - N(t_p)/N_T)$ versus pulse width (t_p) for the E1 and E2 defects in n-InP

should give straight line corresponding to the capture rate, however, the curve is found to be non-linear due to the different capture rates of the free carrier tail extending into the depletion region. The initial part of the plot, which is fairly linear, gives a reliable estimate of the τ_c [58]. The capture rate apparently decreases with time. The possible explanation for this behaviour is the relatively high trap concentration which significantly de

creases the number of electrons available for capture at a later time. The calculated capture cross-section is 3.29×10^{-15} cm^2 for deep level having the activation E1 = 0.29 ± 0.01 eV and 5.85×10^{-17} cm^2 capture cross-section of deep level E2 = 0.69 ± 0.02 eV respectively.

4. CONCLUSIONS

We have investigated the temperature-dependent J–V, C–V characteristics and deep level transient spectroscopy (DLTS) of Ni/V/n-InP Schottky diode. The calculated Schottky barrier height (ϕ_{bo}) and ideality factor (n) of Ni/V Schottky contact is in the range of 0.39 eV and 2.36 at 180 K, and 0.69 eV and 1.27 at 420 K, respectively. It is demonstrated that these anomalies result due to the barrier height inhomogeneities prevailing at the metal–semiconductor interface. The calculated mean barrier height ($\overline{\varphi}_{b0} = 0.95$ eV) and standard deviation ($\sigma_{so} = 128$ eV) clearly indicates the presence of inhomogeneities and potential fluctuation at the interface. Furthermore, the modified $\ln\left(J_0 / T^2\right) - \left(q^2\sigma_{so}^2 / 2k^2T^2\right)$ versus $1000/T$ plot is gives $\overline{\varphi}_{b0}$ and A^* as 0.98 eV and 7.068 AK^{-2}cm^{-2} respectively. The Richardson constant value of 7.068 AK^{-2}cm^{-2} is in close agreement with the known value of 9.4 A.K^{-2}cm^{-2} for n-type InP. It is seen that there is a discrepancy between zero-bias barrier heights (BHs) obtained from J-V and C-V measurements. The discrepancy is especially explained by introducing a spatial distribution of SBHs due to barrier height inhomogeneities that occur at the Ni/V/n-InP interface in the temperature range 180 – 420 K. Based on the DLTS results, two deep level defects are identified (E1 and E2) in as-grown sample, which have activation energies of 0.29 ± 0.01 eV and 0.69 ± 0.02 eV with capture cross-section of 3.29×10^{-15} cm^2 and 5.85×10^{-17} cm^2, respectively. The traps observed at E1 and E2 could be related to V_p related intrinsic donor level and phosphorus antisite defect $P_{in.}$

REFERENCES

1. K. Hattori, Y. Torii, *Solid State Electron.* **34**, 527 (1991).
2. C.W. Wilmsen, Physics and Chemistry of III-V Compound Semiconductor Interfaces (Plenum: New York: 1985).
3. S.M. Sze, Physics of Semiconductor Devices (Second ed., Wiley: New York: 1981).
4. E.H. Rhoderick, Metal–Semiconductor Contacts (Oxford University Press: Oxford: p. 121, 136, 1978).
5. E.H. Rhoderick, R.H. Williams, Metal Semiconductor Contacts (Clarendon Press: Oxford: 1988).
6. H. Cetin, E. Ayyildiz, *Semicond. Sci. Technol.* **20**, 625 (2005).
7. N. Rouag, L. Boussouar, S. Toumi, Z. Ouennoughi, M.A. Djouadi, *Semicond. Sci. Technol.* **22**, 369 (2007).
8. D.M. Kim, D.H. Kim, S.Y. Lee, *Solid State Electron.* **51**, 865 (2007).
9. M.M. El-Nahass, H.M. Zeyada, K.F. Abd-El-Rahman A.A.A. Darwish, *Sol. Energ. Mat. Sol. C.* **91**, 1120 (2007).
10. C.F. Pirri, S. Ferrero, L. Scaltrito, D. Perrone, S. Guastella, M. Furno, G. Richieri, L. Merlin, *Microelectron. Eng.* **83**, 86 (2006).
11. F. Roccaforte, F. La Via, V. Raineri, R. Pierobon, E. Zanoni, *J. Appl. Phys.* **93**, 9137 (2003).
12. R.C. Rossi, N.S. Lewis, *J. Phys. Chem. B* **105 (17)**, 12303 (2001).
13. G.M. Vanalme, L. Goubert, R.L. Van Meirhaeghe, F. Cardon, P. van Daele, *Semicond. Sci. Technol.* **14**, 871 (1999).
14. M.C. Lonergan, F.E. Jones, *J. Chem. Phys.* **115**, 433 (2001).
15. W. Monch, *J. Vac. Sci. Technol. B.* **17**, 1867 (1999).
16. H. Cetin, E. Ayyildiz, *Semicond. Sci. Technol.* **20**, 625 (2005).
17. V. Janardhanam, A. Ashok Kumar, V. Rajagopal Reddy P. Narasimha Reddy, *J. Optoelectron. Adv. Mater.* **2**, 735 (2008).
18. M. Soylu, B. Abay, *Microelectron. Eng.* **86**, 88 (2009).
19. N. Nanda Kumar Reddy, V. Rajagopal Reddy, Optoelectron. Adv. Mater. – Rapid Commun. **4(8)**, 1229 (2010).
20. S. Sankar Naik, V. Rajagopal Reddy, *Superlattice Microst.* **48,** 330 (2010).
21. D. Subba Reddy, M. Bhaskar Reddy, N. Nanda Kumar Reddy, V. Rajagopal Reddy, *J. Mod. Phys.* **2**, 113 (2011).
22. P. Speir, P. Weidmann, W. Kuebart, H. Grossekopf, F. Grotjahn, F. Schuler, F.J. Tegude, K. Wunstel, in: Proceedings of the 5th Conf. Semi-insulating III-V Materials (Sweden, 295, 1988).

23. I.V. Antonova, V.A. Volodin, E.P. Neustroev, S.A. Smagulova, J. Jedrzejewsi, I. Balberg, *J. Appl. Phys.* **106**, 064306 (2009).
24. M. Buljan, J. Grenzer, V. Holy, N. Radic, T. Misic -Radic, S. Levichev, S. Bernstorff, B. Pivac, I. Capan, *Appl. Phys. Lett.* **97**, 163117 (2010).
25. A. Majerfeld, O. Wada, A.N.M.M. Choudhury, *App. Phys. Lett.* **33**, 957 (1978).
26. P.K. Bhattacharya, J.W. Ku, S.J.T. Owen, S.H. Chiao, R. Yeats, *Electron. Lett.* **15**, 753 (1979).
27. S. Guha, F. Hasegawa, *Solid State Electron.* **20**, 27 (1977).
28. J. Bonnafe, M. Castagne, J. Romestan, M. DeMurcia, J.P. Fillard, *Electron. Lett.* **16**, 313 (1980).
29. H. Richard, G. Couturier, A. Chaouki, A.S. Barriere, *J. Appl. Phys.* **62**, 3857 (1987).
30. Y.W. Zhao, Z.Y. Dong, *J. Phys. Chem. Sol.* **69**, 551 (2008).
31. V. Janardhanam, A. Ashok Kumar, V. Rajagopal Reddy, Chel Jong Choi, *Microelectron. Eng.* **88**, 506 (2011).
32. H.K. Henisch, Semiconductor Contacts (Oxford University: London: 1984).
33. R.F. Schmitsdorf, T.U. Kampen, W. Monch, *J. Vac. Sci. Technol. B* **15**, 1221 (1997).
34. T. Kihcoglu, *Thin Solid Films* **516**, 967 (2008).
35. C. Raynaud, K. Isoird, M. Lazar, C.M. Johnson, N. Wright, *J. Appl. Phys.* **91**, 9841 (2002)
36. H. Dogan, N. Yildirim, A. Turut, M. Biber, E. Ayyildiz, C. Nuhoglu, *Semicond. Sci. Technol.* **21**, 822 (2006).
37. N. Newman, M.V. Schilfgaarde, T. Kendelwicz, D.M. Williams, W.E. Spicer, *Phys. Rev. B.* **33**, 1146 (1986).
38. R.T. Tung, *Mater. Sci. Eng. R* **35**, 1 (2001).
39. D.A. Neamen, Semiconductor Physics and Devices (Irwin: Boston: 1992).
40. Zs.J. Horvath, *Solid State Electron.* **39**, 176 (1996).
41. M. Saglam, E. Ayildiz, A. Gumus, A. Turut, H. Efeoglu, S. Tizemen, *Apply. Phys. A,* **62**, 269 (1996).
42. S.K. Cheung, N.W. Cheung, *Appl. Phy. Lett.* **49**, 85 (1986).
43. H.C. Card, E.H. Rheodrick, *J. Appl. Phys. D* **4**, 1589 (1971).
44. J.H. Werner, H.H. Guttler, *J. Appl. Phys* **73**, 1315 (1993).
45. Y.P. Song, R.L. Van Meirhaeghe, W.H. Laflere, F. Cardon, *Solid State Electron.* **29**, 633 (1986).
46. S. Bandyopadyay, A. Bhattacharya, S.K. Sen, *J. Appl. Phys.* **85**, 3671 (1999).
47. S. Zhu, R.L. Van Meirhaeghe, C. Detavernier, F. Cardpn, G.P. Ru, X.P. Qu, B.Z. Li, *Solid State Electron.* **44**, 663 (2000).
48. Y.S. Tsay, G. Gong, S.S. Mitra, *Phy. Rev. B* **6**, 2330 (1972).
49. R.L. Crowell, *Solid State Electron.* **20**, 171 (1977).
50. P. Muret, Ch. Ulzhofer, J. Pernot, Y. Cordier, F, Semond, Ch. Gacquiere, D. Theron, *Superlattice Microst.* **36**, 435 (2004).
51. H. Lim, G. Sagnes, G. Bastide, M. Rouzeyre, *J. Appl. Phys.* **53**, 3317 (1982)
52. S.R. McAfee, F. Capasso, D.V. Lang, A. Hutchirsson, W.A. Bonnor, *J. Appl. Phys.* **52**, 6158 (1981).
53. A. Kadoun, G. Marrakchi, A. Kalboussi, D. Barbier, G. Guillot, *Mater. Sci. Eng. B,* **33**, 188 (1995).
54. Y.W. Zhao, X.L. Xu, M. Gong, S. Fung, C.D. Beling, X.D. Chen, N.F. Sun, T.N. Sun, S.L. Liu, G.Y. Yang, X.B Guo, Y.Z. Sun, L. Wang, Q.Y. Zheng, Z.H. Zhuo, J. Chen, *Appl. Phys. Lett.* **72**, 2126 (1998).
55. Z.Q. Shi, W.A. Anderson, *J. Appl. Phys.* **70**, 3137 (1991).
56. C.V. Reddy. S. Fung, C.D. Beling, *Rev. Sci. Instr.* **67**, 4279 (1996).
57. J.A. Borsuk, R.M. Swanson, *J. Appl. Phys.* **52**, 6704 (1981).
58. H. Indusekhar, V. Kumar, *phys. status solidi A* **95**, 269 (1986).